ResearchGate

See discussions, stats, and author profiles for this publication at: https://www.researchgate.net/publication/6455506

Loop Dynamics and Ligand Binding Kinetics in the Reaction Catalyzed by the Yersinia Protein Tyrosine Phosphatase †

ARTICLE *in* BIOCHEMISTRY · MAY 2007

Impact Factor: 3.02 · DOI: 10.1021/bi602335x · Source: PubMed

CITATIONS
27

READS
18

6 AUTHORS, INCLUDING:

Mazdak Khajehpour
University of Manitoba
24 PUBLICATIONS **384** CITATIONS
SEE PROFILE

li wu
Lanzhou University
62 PUBLICATIONS **2,125** CITATIONS
SEE PROFILE

All in-text references underlined in blue are linked to publications on ResearchGate, letting you access and read them immediately.

Available from: Mazdak Khajehpour
Retrieved on: 28 January 2016

Loop Dynamics and Ligand Binding Kinetics in the Reaction Catalyzed by the *Yersinia* Protein Tyrosine Phosphatase†

Mazdak Khajehpour,*,‡ Li Wu,§ Sijiu Liu,§ Nick Zhadin,‡ Zhong-Yin Zhang,§ and Robert Callender‡

Department of Biochemistry, Albert Einstein College of Medicine, 1300 Morris Park Avenue, Bronx, New York 10461, and Department of Biochemistry and Molecular Biology, Indiana University School of Medicine, 635 Barnhill Drive, Indianapolis, Indiana 46202-5122

Received November 13, 2006; Revised Manuscript Received January 31, 2007

ABSTRACT: The *Yersinia* protein tyrosine phosphatase (YopH) contains a loop of ten amino acids (the WPD loop) that covers the entrance of the active site of the enzyme during substrate binding. In this work the substrate mimicking competitive inhibitor *p*-nitrocatechol sulfate (PNC) is used as a probe of the active site. The dynamics of the WPD loop was determined by subjecting an equilibrated system containing YopH, PNC, and YopH bound to PNC to a laser induced temperature jump, and subsequently following the change in equilibrium due to the perturbation. Using this methodology the dynamics associated with substrate binding in YopH have been determined. These results indicate that substrate binding is coupled to the WPD loop motion, and WPD loop dynamics occur in the sub-millisecond time scale. The significance of these dynamic results is interpreted in terms of the catalytic cycle of the enzyme.

Protein tyrosine phosphatases (PTPs[1]) are a large and structurally diverse family of signaling enzymes that together with protein tyrosine kinases modulate the cellular level of tyrosine phosphorylation (*1*−*6*). Defective or inappropriate regulation of PTP activity leads to aberrant tyrosine phosphorylation, which contributes to the development of many human diseases including cancers and diabetes (*7*). The *Yersinia* PTP (YopH, Figure 1) is essential for virulence of the bacteria responsible for the plague, and it is the most active PTP known to date. The bacteria produce this enzyme aiming solely to interfere with the host signaling process; deleting the genes associated with YopH production only affects the propagation of the bacterium in the host (*8*).

The high activity of YopH has made it a model system for detailed mechanistic studies of the PTPs (*9*). Site-directed mutagenesis combined with detailed kinetic and mechanistic studies of *Yersinia* PTP using the unnatural substrate PNPP (Figure 2a) and other substrates have contributed greatly to the understanding of the chemical mechanism for PTP catalysis, the nature of the enzymatic transition state, and the means by which the transition state is stabilized (*2*, *7*, *9*−*21*). From these studies it is understood that PTPs share a common catalytic mechanism to effect catalysis. A Cys nucleophile (Cys403 in the *Yersinia* PTP) is utilized in the formation of a thiophosphoryl covalent enzyme intermediate E-P. The invariant Arg residue (Arg409 in the *Yersinia* PTP) functions in substrate binding and in transition state stabilization. The initial phosphoryl transfer step is assisted by the conserved Asp (Asp356 in the *Yersinia* PTP) which protonates the leaving group thereby acting as a general acid catalyst. The phosphoenzyme intermediate E-P undergoes hydrolysis in a second step, which is catalyzed by the same Asp356 acting as a general base. YopH has two structural domains, the N-terminal domain consisting of residues 1−129 (*22*), and the catalytic domain consisting of residues 163−468 (Figure 1) (*20*). The crystal structure of both domains has been solved separately, but the total protein has not yet been crystallized (*15*, *16*, *23*).

The crystal structures suggest that the WPD loop in the *Yersinia* PTP has two distinct conformations (Figure 1). Crystallographic and UV−resonance Raman spectral evidence indicate that in solution, for the ligand-free enzyme, the WPD loop exists in two conformations having similar thermodynamic stability: the "open" conformation in which there is negligible interaction between the WPD loop and the P-loop, and a "closed" conformation that is very similar to that adopted by the ligand-bound form of the enzyme (*11*). In the ligand-bound enzyme form, the WPD loop adopts a "closed" state and Asp356 on the WPD loop makes a hydrogen bond with the ligand. Therefore upon substrate binding, the loop folds over the active site to position the Asp residue close to the scissile oxygen of the substrate for efficient proton transfer.

In contrast to our understanding of the structures and chemical mechanism, very little is known about the dynamics associated with the substrate binding and catalysis of the YopH enzyme. Many enzymes are characterized by fluctuating conformations and dynamic motions which are coupled to the binding and release of substrate or product (*24*, *25*). Such conformational change and motion may function to exclude solvent, recruit essential amino acids for catalysis or to stabilize and/or prevent loss of reactive intermediates

† This work was supported by National Institutes of Health Grant CA69202 (Z.Y.Z.) and National Institutes of Health Grants 5P01GM068036 and EB01958 (R.C.).

* To whom correspondence should be addressed. Tel: 718-430-2961. Fax: 718-430-8666. E-mail: mazdak@medusa.bioc.aecom.yu.edu.

‡ Albert Einstein College of Medicine.

§ Indiana University School of Medicine.

[1] Abbreviations: YopH, *Yersinia* outer membrane protein; YopHΔ162, the catalytic domain of YopH; PNPP, *p*-nitrophenyl phosphate; PNC, *p*-nitrocatechol sulfate; PTP, protein tyrosine phosphatase.

10.1021/bi602335x CCC: $37.00 © 2007 American Chemical Society
Published on Web 03/13/2007

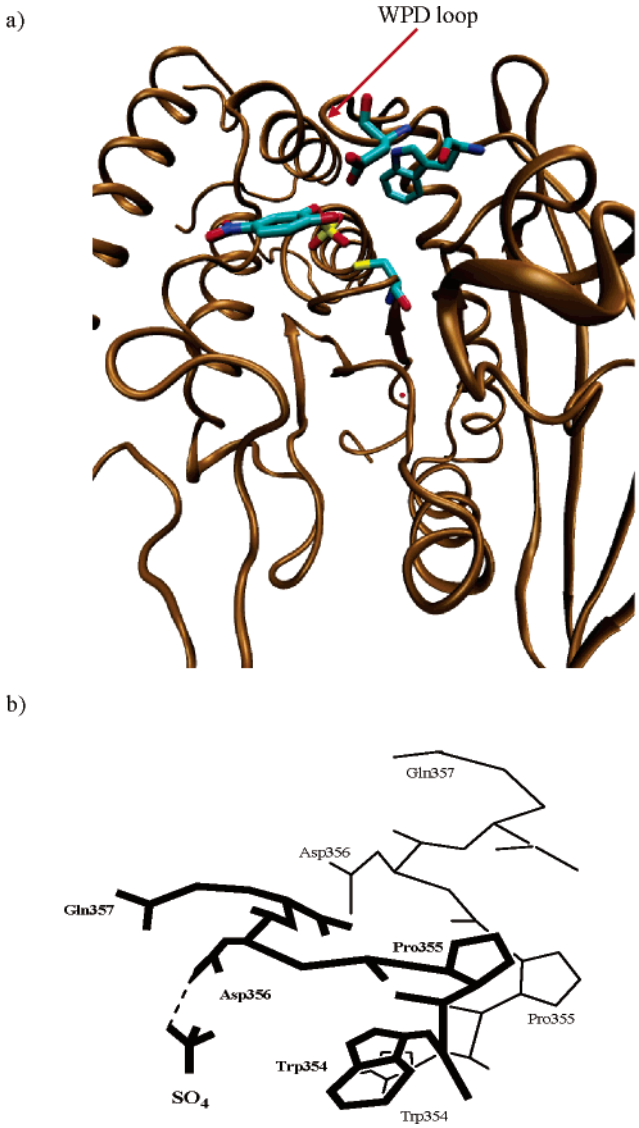

FIGURE 1: (a) Crystal structure of YopHΔ162 complexed with PNC (*p*-nitrocatechol sulfate), showing the tryptophan and aspartic acid and cysteine residues. (b) Representation of the two conformations of the WPD loop relative to the sulfate group of PNC, the open conformation (thin line) and the closed conformation (thick line).

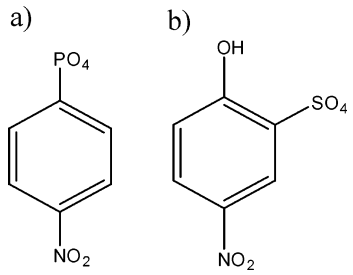

FIGURE 2: Chemical structure of (a) PNPP (*p*-nitrophenyl phosphate) and (b) PNC (*p*-nitrocatechol sulfate).

(*26*−*38*). For PTPs, the conformational change associated with ligand binding is restricted to the movement of a flexible loop that has been described as a hinged loop movement (*4*, *15*, *39*). This loop, termed the WPD loop, harbors the essential general acid/base (Asp356 in the *Yersinia* PTP).

To probe the dynamics of the protein we have employed temperature jump relaxation spectroscopy. This methodology was originally developed by Eigen (*40*−*43*) and was applied to enzymes by Hammes and other researchers (*44*−*51*). The method relies upon the fact that the binding and release of a ligand to an enzyme depends upon the enzyme's dynamics. Therefore, by thermally perturbing and subsequently monitoring the relaxation of an enzyme−ligand system to new equilibrium values, it is possible to obtain kinetic information about the dynamic processes occurring in the enzyme.

These classical T-jump methodologies effect the temperature perturbation by discharging a large electrical current into the protein solution; the dead-time of these methods was around 10−20 μs. The dead-time is significantly reduced by employing IR lasers as the temperature perturbing agent. This method allows the dynamic nature of proteins to be monitored over a large time range stretching from nanoseconds to tens of milliseconds, and we previously have demonstrated the versatility of applying laser-induced T-jump spectroscopic methods for measuring dynamic processes in enzymes (*33*−*38*, *52*, *53*).

The *Yersinia* PTP provides a unique system to address the dynamics of the WPD loop using fluorescence as a probe; it contains only one tryptophan residue, Trp354, which is invariant among all PTPs, and this residue is located on the same flexible WPD loop as is the putative general acid Asp356. The spectral properties of this lone tryptophan can be used to monitor the dynamics of the WPD loop. This work determines the WPD loop opening and closing rates in the catalytic domain of YopH (YopHΔ162) using *p*-nitrocatechol sulfate (PNC, Figure 2b) as a substrate mimic ligand. This molecule has a structure similar to PNPP and is a competitive inhibitor of YopH (*16*). In addition, PNC drastically quenches the tryptophan fluorescence of the WPD loop when it binds to the active site of the enzyme. These properties make PNC an excellent probe for monitoring the dynamic processes occurring at the active site of YopH.

MATERIALS AND METHODS

Materials. PNC was purchased from Aldrich (Milwaukee, WI). The catalytic domain of the *Yersinia* protein tyrosine phosphatase (YopHΔ162) was expressed and purified as described previously (*15*, *20*). Unless otherwise noted all experiments were done in pH 6.5 sodium citrate/sodium chloride buffer at an ionic strength of 0.15.

Methods. *Fluorescence Spectroscopy*. Steady-state fluorescence spectra were measured on a FluoroMax-2 spectrofluorimeter (Instruments S. A. Group, Edison, NJ) with a spectral resolution of 3 nm for both excitation and emission. A sample was held in a 1 × 10 mm quartz cuvette and excited along the short dimension. The wavelength of excitation was 290 nm for all measurements. Contributions to the emission spectra from the Raman scattering bands of the solvent were corrected by subtracting a solvent blank taken under identical conditions as the sample. The fluorescence spectra were also corrected for instrument spectral response using an instrument correction factor. The data was analyzed with Sigmaplot (Point Richmond, CA) software.

The dissociation constant, K_d, of PNC from YopHΔ162 was determined by monitoring changes in the fluorescence intensity, as unligated YopHΔ162 was titrated with increasing amounts of PNC. For a fluorescence monitored titration,

ΔF varies with the PNC concentration, [PNC], according to the following equation (*54*):

$$\text{fraction bound} = \frac{\Delta F}{\Delta F_{max}} = \frac{[\text{PNC}]}{\{[\text{PNC}] + K_d\}} \quad (1)$$

ΔF_{max} is the change in the signal when all enzyme is bound to the inhibitor.

T-Jump Measurement. The instrument used to measure relaxation kinetics is based on the same principles as described previously (*33*, *35*, *36*). Temperature jumps were induced by exposing a volume of water to a pulse of infrared light (1.56 μm wavelength, 90−120 mJ energy, 1.5−2.0 mm diameter spot on the sample, 0.5 mm path length), generated by stimulated Raman shifting the fundamental emission (1.064 μm) of a Powerlite 7010 Q-switched Nd:YAG laser (Continuum, Santa Clara, CA), operating at 2 Hz, in a 1 m long cell filled with deuterium gas at 650 psi. Water absorbed the laser energy, and the temperature of the exposed volume increased in approximately 6 ns. The size of the T-jump was calibrated using the change of water IR absorption with temperature. Typical T-jump values ranged from 6.5 to 8.5 °C. Diffusion of heat out of the interaction volume proceeds with a time constant of approximately 35 ms. Hence, the apparatus generated a T-jump within 6 ns that remained nearly constant until approximately 10 ms.

To probe changes in the fluorescence intensity of the tryptophan fluorophore, the sample was irradiated by a group of emission lines near 290 nm from an Innova 200-25/5 argon ion laser (Coherent, Palo Alto, CA). To avoid photodamage to the sample, the excitation light was modulated using a shutter that allowed 12 ms exposure for every T-jump pulse. Also, power of the excitation beam was attenuated by neutral density filters; typical beam intensity was 15−20 mW. The incident excitation beam is focused onto a 0.3 mm diameter spot on the sample, in the center of the beam path of the 1.56 μm pulse. Tryptophan fluorescence emission, detected at 50° to the excitation beam, was passed through a narrow band filter (340 ± 12 nm) and was monitored using a R4220P photomultiplier tube (Hamamatsu, Bridgewater, NJ). Data were digitized with a CS82G data acquisition board (Gage applied technologies, Montreal, Quebec, Canada) at 1 GS/s sampling rate. Overall temporal resolution of the system is about 20 ns. A background signal obtained without fluorescence excitation was measured separately and subtracted from the kinetic data. A program written in LabVIEW (National Instruments, Austin, TX) was used for instrument control and data collection. Data were normalized to the average fluorescence intensity taken before the T-jump.

In short, T-jump relaxation profiles are obtained by subjecting the sample to a laser-induced temperature jump every 500 ms. The relaxation is monitored using fluorescence for the first 7 ms after the T-jump; once 300 ms has elapsed, the sample has relaxed to its original temperature, allowing the T-jump to be repeated. Each relaxation curve contains data from performing 3600 temperature jumps upon the same sample. Curve fitting was done with Sigmaplot (Point Richmond, CA) software. The uncertainties in the reported values of relaxation rates were determined from the fitting parameters.

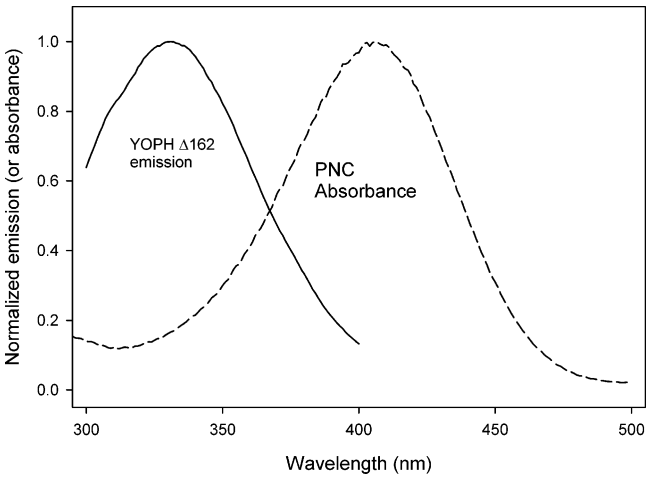

FIGURE 3: Comparing the emission spectrum of YopHΔ162 with the absorbance of PNC. Conditions for emission spectrum: 5 μM YopHΔ162, pH 6.5 citrate buffer at 0.15 ionic strength adjusted by NaCl, excitation 285 nm excitation and emission slits set at 5 nm bandpass, the spectrum is normalized to maximum emission at 330 nm. Conditions for absorbance spectrum: pH citrate buffer at 0.15 ionic strength adjusted by NaCl, the spectrum is normalized to the maximum absorbance at 405 nm having an ϵ_{max} of 18150 M^{-1} cm^{-1} (*61*).

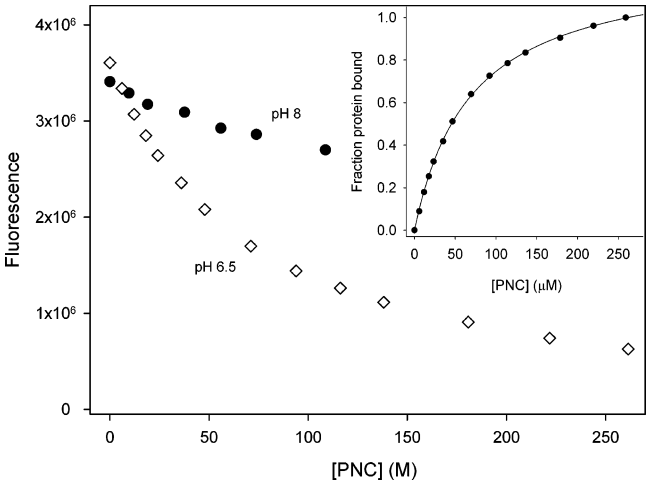

FIGURE 4: Fluorescence intensity of YopHΔ162 measured at 330 nm (excitation 285 nm, 5 nm slits) as a function of PNC concentration at two different pH values. The inset plots the binding curve as defined by eq 2, for binding of PNC to YopHΔ162 at pH 6.5. The total concentration of protein is 5 μM.

RESULTS

Equilibrium Measurement Results. Figure 3 depicts the emission spectrum of YopHΔ162 and the absorbance spectrum of PNC. The Förster distance R_0 can be obtained using Figure 3 and eq 2 (*55*). We estimate R_0 to be

$$R_0 = 0.211[\kappa^2 n^{-4} Q_D J(\lambda)]^{1/6} \quad (2)$$

approximately 24 ± 7 Å; this value is not very sensitive to fluctuations in quantum yield. The distance between the tryptophan of YopHΔ162 and the enzyme-bound PNC is much less than this Förster distance value (*16*); therefore the quenching efficiency of enzyme-bound PNC is almost 100%.

Figure 4 plots the fluorescence intensity of YopHΔ162 measured at 330 nm as a function of PNC concentration at

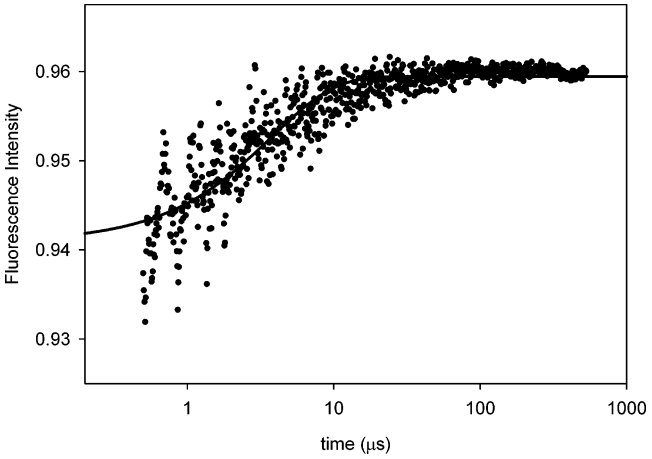

FIGURE 5: T-Jump fluorescence relaxation profiles of apo-YopHΔ162. The sample was 34 μM in YopHΔ162 and buffered at pH 6.5 with ionic strength of 0.15 in NaCl.

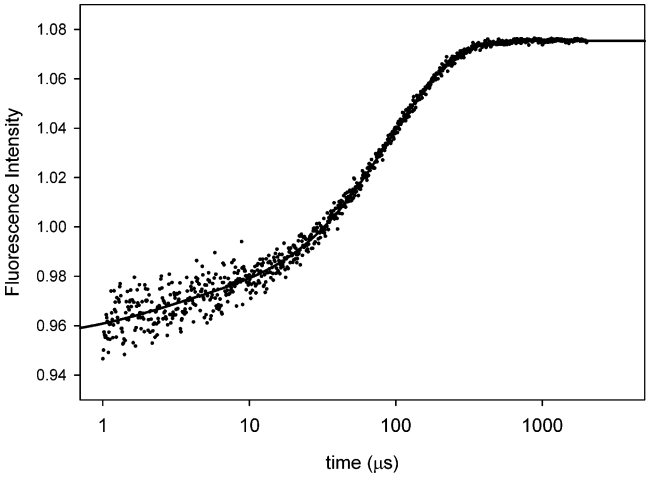

FIGURE 6: T-jump fluorescence relaxation profiles of YopHΔ162 at different concentrations of PNC. The sample was 18 μM in YopHΔ162 and buffered at pH 6.5 with ionic strength of 0.15 in NaCl. The sample was excited at 290 nm and the emission was collected at 340 nm as described in Materials and Methods.

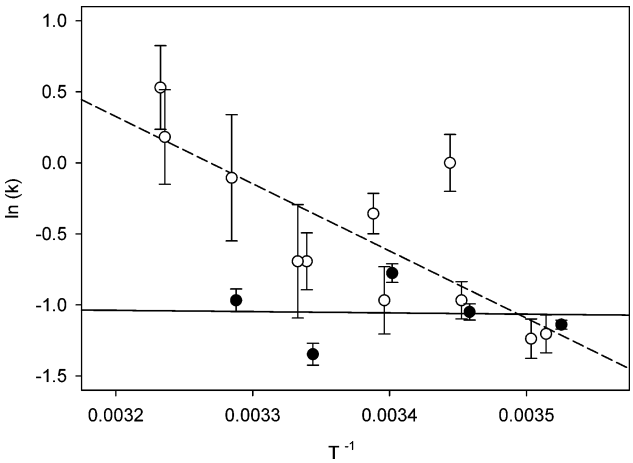

FIGURE 7: The temperature dependence of the relaxation rates k_1(obs) and $(\tau_{apo})^{-1}$. The k_1(obs) data are represented by the open circles and are linearly correlated with the dashed line. The $(\tau_{apo})^{-1}$ data are shown by the closed circles and are linearly correlated by the solid line. For k_1(obs) the experimental conditions are similar to those of Figure 6; the PNC concentration is 52, 83, 102, 210 μM. For $(\tau_{apo})^{-1}$ the experimental conditions are those of Figure 5.

25 °C. The binding of the ligand to the enzyme is characterized by quenching of the enzyme fluorescence. The fluorescence quenching profiles are pH dependent. At pH 8 minimal quenching occurs, indicating that either PNC does not bind the enzyme or it binds the enzyme at a site far (i.e., greater than 24 Å) from the active site. Hence, PNC can only function as a probe of the active site at pH values less than 7. The pH dependence of the binding is not due to changes in ligand ionization, as we have not observed any changes in the absorbance spectrum of the ligand as the pH is changed from 8 to 6. However, studying the X-ray crystal structure of PNC−YopHΔ162 demonstrates that there are two hydrogen bonds between the general acid Asp 356 and PNC; this might be responsible for the loss of binding at pH values higher than 7. From the fluorescence intensities the binding constant can be determined from fitting the data to eq 3; this is demonstrated in the inset of Figure 4. The values of K_d corresponding to the temperatures of 10, 18, 23, and 31 °C are respectively 30 ± 10 μM, 59 ± 5 μM, 110 ± 16 μM, and 130 ± 15 μM. The binding of PNC to YopHΔ162 is exothermic therefore a temperature jump will cause some of the enzyme-bound ligand to dissociate, leading to an increase in fluorescence.

T-Jump Results. Figure 5 depicts the fluorescence relaxation profile of the apo-YopHΔ162 system after T-jump. We obtain a very low amplitude monoexponential relaxation with a time constant of approximately 3 μs. They exhibit a rather flat temperature dependence given by the equation $\ln(\tau_{apo}^{-1}) = -0.75 - [91/T(\mathrm{K})]$; this correlation is later shown in Figure 7. It is difficult to unequivocally assign this relaxation. Previous resonance Raman measurements demonstrate that two different WPD loop conformations exist under normal conditions and that they have similar stability. For this reason, and because our spectroscopic monitor (the indole ring of the protein's only tryptophan residue) lies within the WPD loop, we propose that this observed relaxation is due to a conformational change associated with loop opening and closing. Consider the following equilibrium existing in the apoprotein system:

$$E_{open}^{apo} \underset{k(apo)_{open}}{\overset{k(apo)_{close}}{\rightleftharpoons}} E_{close}$$

The inverse of the relaxation time observed in the apoprotein τ_{apo}^{-1} will be the sum of $k(apo)_{close}$ and $k(apo)_{open}$. Studying this motion in the apoprotein system, using T-jump UV−resonance Raman spectroscopy (which can discern geometrical shifts of the indole ring), is the focus of future work.

Examples of fluorescence relaxation profiles of the YopHΔ162−PNC system after T-jump are given in Figure 6. These relaxation profiles are biexponential in time having the form of eq 3.

$$I = A_1 \exp[1 - k_1(\mathrm{obs})t] + A_2 \exp[1 - k_2(\mathrm{obs})t] \quad (3)$$

The fast time constant, $(k_1(\mathrm{obs}))^{-1}$, is in the order of a few microseconds while the slow time constant, $(k_2(\mathrm{obs}))^{-1}$, is in the order of a few hundred microseconds. Accurately determining the fast relaxation rate is difficult due to high

Table 1: Fitting Parameters Obtained by Fitting k_2(obs) to the Equation $\ln(k) = A - (B/T)$

total concn of PNC and YopHΔ162 (μM)	A	B	r^2
16	10.36	4441	0.985
55	9.49	4129	0.999
82	9.82	4176	0.999
102	8.33	3711	0.999
202	7.69	3406	0.999
305	7.30	3210	0.999
616	7.84	3252	0.931
883	9.35	3670	0.977
1600	13.41	4808	0.82

Scheme 1

$$E_{open}^{apo} \underset{k(apo)_{open}}{\overset{k(apo)_{close}}{\rightleftharpoons}} E_{close}$$

$$E_{open}^{apo} + L \underset{k_{off}}{\overset{k_{on}}{\rightleftharpoons}} E_{open} \bullet L \underset{k_{open}}{\overset{k_{close}}{\rightleftharpoons}} E_{close} \bullet L$$

noise levels existing in the nanosecond to microsecond region of the relaxationprofiles. Reasonably accurate and precise values for this parameter have only been obtained for total (YopHΔ162 + PNC) concentrations of 52, 83, 102, and 210 μM; these conditions had maximum signal-to-noise ratios. Under these conditions, k_1(obs) demonstrated no concentration dependence; however k_1(obs) exhibits temperature dependence as shown in Figure 7, which may be expressed by the equation $\ln(k_1(\text{obs})) = 15.48 - [4736/T(\text{K})]$. As shown in Figure 7 this relaxation can be distinguished from that of the apoenzyme as the apoenzyme relaxation exhibits much smaller temperature dependence.

The slow relaxation step is highly resolved, and when the total concentration of PNC is fixed, the apparent rate constant k_2(obs) follows Arrhenius behavior. We have tabulated the temperature dependence of different k_2(obs) in Table 1 in terms of Arrhenius fit parameters from the raw data. For subsequent analysis we use values interpolated from the equations. Figure 8 plots the concentration dependence of k_2(obs) at different isotherms. This rate constant shows concentration dependence.

The simplest model describing the binding process of PNC to YopHΔ162 is given in Scheme 1. In this mechanism, E is the enzyme, L is the ligand, k_{on} and k_{off} are the ligand on and off rates, and k_{open}, k_{close}, $k(\text{apo})_{open}$, and $k(\text{apo})_{close}$ are the rates of conformational change associated with opening and closing of the WPD loop in the ligand bound and apoenzyme situations.

Three relaxation times are predicted by this kinetic scheme τ_1, τ_2, and τ_3. The relaxation involving k_{open} and k_{close} is much slower than the other processes; therefore the kinetics can be solved assuming that this step is decoupled from the initial two steps. The following expressions for the three time constants τ_1, τ_2, and τ_3 are obtained (*56*). The slow time constant τ_3 is obtained from eq 4.

$$\tau_3^{-1} = \frac{k_{close}([E] + [L])}{([E] + [L]) + \frac{k_{off}}{k_{on}}\left(1 + \frac{k(\text{apo})_{close}}{k(\text{apo})_{open}}\right)} + k_{open} \quad (4)$$

From UV−resonance Raman measurements performed upon the apoprotein, the protein conformations associated with the open and closed loop forms have similar stability(*11*), allowing us to assume that $k(\text{apo})_{close} \approx k(\text{apo})_{open}$, and eq 4 can be rewritten as

$$\tau_3^{-1} \approx \frac{k_{close}([E] + [L])}{([E] + [L]) + \frac{k_{off}}{k_{on}}(2)} + k_{open} \quad (4a)$$

In this case [E] is the total concentration of free enzyme and [L] is the concentration of ligand. We have performed stopped-flow experiments upon the PNC−YopHΔ162 system, and we have not detected any binding processes occurring slower than a millisecond. Therefore $(k_2(\text{obs}))^{-1}$ is considered to be τ_3; and, from fitting the data in Figure 8 to eq 4, the constants k_{close} and k_{open} and k_{off}/k_{on} can be directly determined. The lines in Figure 8 depict the best fit of eq 4 through each set of isothermal data. The results are well correlated with the equation. We have tabulated all the fitting results in Table 2. The microscopic rate constants k_{open}, k_{close}, and k_{off}/k_{on} are obtained directly from the fits.

Since the first two steps are effectively decoupled from $(t_3)^{-1}$, the time constants τ_1 and τ_2 are obtained from eqs 5 and 6 (*56*).

$$\tau_1^{-1} + \tau_2^{-1} = k(\text{apo})_{open} + k(\text{apo})_{close} + k_{off} + k_{on}([E_{open}^{apo}] + [L]) \quad (5)$$

$$\frac{1}{\tau_1\tau_2} = k_{off}(k(\text{apo})_{open} + k(\text{apo})_{close}) + k_{on}\{k(\text{apo})_{open}([E_{open}^{apo}] + [L]) + k(\text{apo})_{close}[E_{open}^{apo}]\} \quad (6)$$

Our relaxation curves for the measurements with ligand present demonstrate biexponential kinetics instead of three exponentials as would be inferred from Scheme 1. This may be either because our first relaxation process is too fast for detection or because the two relaxation times are rather close and cannot be resolved at the existing signal-to-noise ratios.

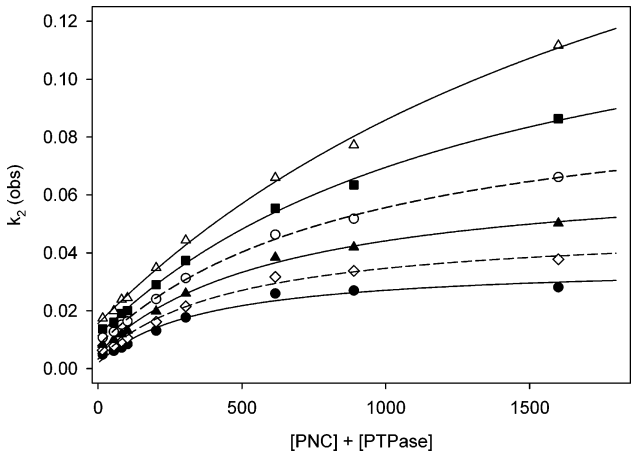

FIGURE 8: The concentration dependence of k_2(obs) at different isotherms. The temperatures are 10 °C (full circle), 15 °C (open diamond), 20 °C (full triangle), 25 °C (open circle), 30 °C (full square), and 35 °C (open triangle). In all cases the conditions are those of Figure 6. The correlation lines are obtained by fitting the data in each isotherm to eq 4.

Table 2: Microscopic Kinetic Parameters Associated with the Suggested Binding Mechanism of PNC to YopHΔ162, as Delineated by Scheme 1[a]

kinetic and thermodynamic parameters	10 °C	15 °C	20 °C	25 °C	30 °C	35 °C
k_{open} $(\mu s)^{-1}$	0.002 ± 0.001	0.003 ± 0.001	0.0053 ± 0.0009	0.0080 ± 0.0008	0.01114 ± 0.0008	0.016 ± 0.001
k_{close} $(\mu s)^{-1}$	0.034 ± 0.003	0.046 ± 0.003	0.064 ± 0.003	0.091 ± 0.004	0.139 ± 0.009	0.23 ± 0.02
$(k_{off}/k_{on})\{1 + [k(apo)_{close}/k(apo)_{open}]\}$ $(\mu M)^{-1}$	400 ± 100	500 ± 100	640 ± 90	900 ± 100	1400 ± 200	2300 ± 400
k_1(obs) $(\mu s)^{-1}$	0.3 ± 0.4	0.4 ± 0.4	0.5 ± 0.2	0.7 ± 0.5	0.9 ± 0.6	1.1 ± 0.9
$k_{off} + k_{on}([E] + [L])$ $(\mu s)^{-1}$	0.2 ± 0.4	0.4 ± 0.4	0.6 ± 0.2	1.0 ± 0.5	1.4 ± 0.6	1.8 ± 0.9
k_{off} $(\mu s)^{-1}$	0.1 ± 0.2	0.3 ± 0.3	0.5 ± 0.2	0.8 ± 0.4	1.2 ± 0.5	1.7 ± 0.8
k_{on} $(M^{-1}\ s^{-1})/10^9$	0.5 ± 1.0	1.0 ± 1.0	1.6 ± 0.6	1.8 ± 0.9	1.7 ± 0.7	1.5 ± 0.7
$K_{loop} = k_{open}/k_{close}$	0.06 ± 0.03	0.07 ± 0.02	0.08 ± 0.01	0.09 ± 0.01	0.082 ± 0.008	0.07 ± 0.007
$(k_{off}/k_{on})\{1 + [k(apo)_{close}/k(apo)_{open}]\} \times (k_{open}/k_{close})$	24 ± 13	35 ± 12	51 ± 10	81 ± 13	120 ± 20	160 ± 32

[a] These parameters are obtained from analyzing the data in Figures 7 and 8 via the methodology laid out in the Results section.

In the case of the first scenario (first relaxation process is too fast), we have the following expression (*56*):

$$\tau_2^{-1} = k_1(\text{obs}) = k(\text{apo})_{\text{open}} + \frac{k(\text{apo})_{\text{close}}}{1 + \dfrac{[\text{I}]}{[\text{E}^{\text{apo}}_{\text{open}}] + \dfrac{k_{\text{off}}}{k_{\text{on}}}}} \quad (7)$$

Equation 7 predicts that k_1(obs) exhibits a hyperbolic dependence upon the concentration of inhibitor and in all cases $\{(\tau_{apo})^{-1} = k(apo)_{open} + k(apo)_{close}\} \geq k_1(obs)$. Judging from Figure 7, the values of k_1(obs) are significantly larger than $(\tau_{apo})^{-1}$ and demonstrate a different temperature dependence. This argues against the first scenario.

The second scenario postulates that k_1(obs) is a combination of τ_1 and τ_2. Since τ_1 and τ_2 are within an order of magnitude of each other, as a first approximation we may assume that k_1(obs) ≈ average (τ_1 and τ_2). In this case, we rewrite eq 5 as

$$\tau_1^{-1} + \tau_2^{-1} = 2k_1(\text{obs}) = k(\text{apo})_{\text{open}} + k(\text{apo})_{\text{close}} + k_{\text{off}} + k_{\text{on}}([\text{E}^{\text{apo}}_{\text{open}}] + [\text{L}]) \quad (8)$$

By rearranging eq 8 we obtain

$$k_{\text{off}} + k_{\text{on}}([\text{E}^{\text{apo}}_{\text{open}}] + [\text{L}]) \approx 2k_1(\text{obs}) - \tau_{\text{apo}}^{-1} \quad (9)$$

In principle, from eqs 9 and 4a all four microscopic rate constants can be obtained.

The k_1(obs) values tabulated in Table 2 are obtained from the regression line in Figure 7; the uncertainties are based upon a confidence level of ninety percent. The insensitivity relative to concentration observed in the data in Figure 7 is due to the fact that the variation in the $k_{on}([E^{apo}_{open}] + [L])$ term is not large compared to the uncertainty in the data. However we can calculate k_{on} and k_{off} by using the values of k_{off}/k_{on} in conjunction with the values of k_1(obs) obtained in Table 2 and eq 9. Since the values of k_1(obs) are obtained from the correlating the data in Figure 7, we can calculate k_{off} from eq 9 by assuming $([E^{apo}_{open}] + [L])$ to be 110 ± 68 μM (this value varies from 52 to 210 μM) and subsequently propagate the uncertainty associated with this assumption in the resulting k_{off} and k_{on} values. These values are reported in Table 2.

The rate constant k_{on} fluctuates around 1×10^9 M^{-1} s^{-1}, which is very close to the diffusion limit (*25*). We have calculated the parameters k_{open}/k_{close}, k_{off}/k_{on}, and K_d. The value of k_{open}/k_{close} is approximately 0.075, indicating that, when PNC is bound to the enzyme, the population of the closed form is more than 10 times that of the open. This is in contrast with the apo form, for which the populations of the two forms are equal (*11*).

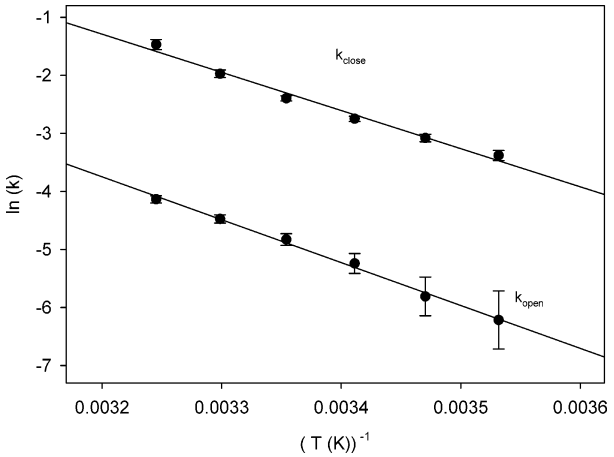

FIGURE 9: The temperature dependence of the microscopic rate constants k_{close} and k_{open}. The correlation equations are $\ln(k_{close}) = (20 \pm 1) - (6100 \pm 400)T^{-1}$ and $\ln(k_{open}) = (19.9 \pm 0.9) - (7500 \pm 300)T^{-1}$.

Figure 9 depicts the temperature dependence of the opening and closing rate constants. From this we obtain the following correlations:

$$\ln(k_{close}) = (20 \pm 1) - (6600 \pm 400)T^{-1}$$
$$(\Delta H^{\ddagger})_{close} = 13.1 \pm 0.7 \text{ kcal mol}^{-1}$$

$$\ln(k_{open}) = (19.9 \pm 0.9) - (7400 \pm 300)T^{-1}$$
$$(\Delta H^{\ddagger})_{open} = 14.7 \pm 0.6 \text{ kcal mol}^{-1}$$

An enthalpy difference of 1.6 ± 0.9 kcal mol^{-1} exists between the two "open" and "closed" states (if we assume a two state transition). From the pre-exponential factor a $(\Delta S^{\ddagger})_{open} \approx (\Delta S^{\ddagger})_{close} \approx -19 \pm 1$ cal mol^{-1} K^{-1} is obtained.

The mechanism outlined in Scheme 1 allows the K_d to be calculated from the T-jump data, $K_d = (k_{off}/k_{on})\{1 + [k(apo)_{close}/k(apo)_{open}]\}(k_{open}/k_{close})$. These values are tabulated in Table 2. As seen in Figure 10, the K_d values from T-jump and the values obtained from steady-state fluorescence measurements are quite close to one another. This fact, in

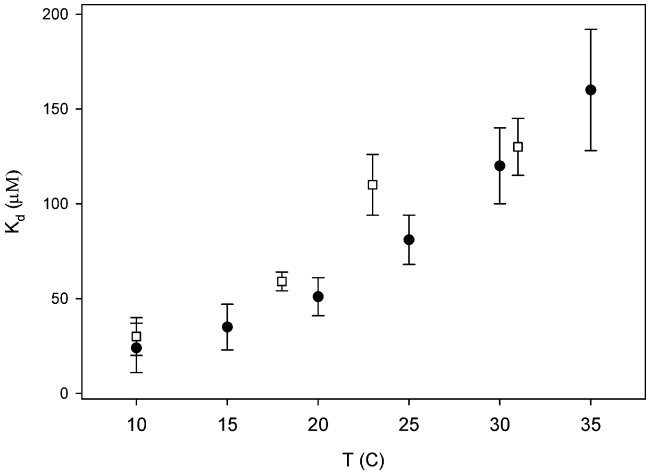

FIGURE 10: Comparing K_d obtained from steady-state fluorescence measurement (open squares) with those from T-jump measurements (full circles).

Scheme 2

$$E + S \underset{k_{off}}{\overset{k_{on}}{\rightleftharpoons}} [ES_{open}] \underset{k_{open}}{\overset{k_{close}}{\rightleftharpoons}} [ES_{close}] \xrightarrow{k_2} [E - P_i] + Y \xrightarrow{k_3} E + S$$

addition to the fact that k_{on} approaches the diffusion limit, demonstrates that our kinetic scheme seems complete.

DISCUSSION

PNC is a ligand that closely mimics PNPP, a small substrate used to probe the catalytic cycle of protein tyrosine phosphatase enzymes. Based upon crystallographic data, the binding of PNC to YopHΔ162 induces a conformation change in the WPD loop of enzyme causing the enzyme to adopt a "closed loop" structure (*16*). We have used PNC as a probe to monitor the dynamics of substrate binding to YopHΔ162.

The T-jump relaxation data of the (YopHΔ162)−PNC system indicates that the simplest model describing the binding of small substrates to the enzyme is a two-step model outlined in Scheme 1. An analysis of the data indicates that our kinetic scheme seems complete, because, first, we obtain a k_{on} value that is close to the diffusion limit; second, our T-jump and steady-state estimations of K_d are in agreement; and finally, we have not observed any relaxations occurring slower than a millisecond. Therefore, it is likely that small substrates bind to YopHΔ162 via this two-step model.

The catalytic cycle is represented in Scheme 2, as suggested by Hengge and Zhang (*17*, *21*). In this scheme, E is the apoenzyme and ES_{open} and ES_{close} are enzyme conformations associated with the open and closed forms of the WPD loop.

Based upon the T-jump data we can characterize the substrate binding steps. From Table 2 the dynamic parameters are $k_{on} \sim 10^9$ M^{-1} s^{-1}, $k_{off} \sim (0.1 \times 10^6$ to 2×10^6 $s^{-1})$, $k_{close} \sim (3 \times 10^4$ to 2×10^5 $s^{-1})$, and $k_{open} \sim (2 \times 10^3$ to 2×10^4 $s^{-1})$. From stopped-flow measurements the values of k_2 and k_3 are measured to be approximately 400 s^{-1} and 100 s^{-1}. These values definitely demonstrate that the enzyme dynamic processes involved in substrate binding are much faster than the subsequent chemical steps. Maximum turnover of PNPP measured at 30 °C and pH 6.5 yields a k_{cat} of approximately 100 s^{-1} (*57*).

The transition state of the dephosphorylation of the tyrosine phosphate (step k_2) has been characterized using kinetic isotope methods; judicious isotope substitutions in PNPP cause kinetic isotope effects that can be measured by the steady-state kinetic analysis of protein tyrosine phosphatase enzymes (*17*, *58*). These experiments indicate that, during the hydrolysis of PNPP, significant commitment factors are absent up to the formation of the phosphoenzyme. We can verify this by calculating the forward commitment factor for the hydrolysis of PNPP by YopHΔ162 from the expression $(k_2/k_{open})[1 + (k_{close}/k_{off})]$ using our T-jump data; from this we conclude that our commitment factor will not exceed 0.2. This low value for the commitment factor is consistent with what is suggested from the kinetic isotope effect results measured for the enzymatic hydrolysis of PNPP.

As we have pointed out before, the rate constants k_{open} and k_{close} are rates of enzyme conformational changes associated with loop opening and closing. The active site of YopHΔ162 is located near the surface of the protein (*15*); in addition, PNC is a small ligand. Therefore judging from the crystal structure of the YopHΔ162−PNC complex, the structural perturbation caused by PNC binding is confined to the active site of the enzyme; the most significant perturbation is observed in the WPD loop (*16*). Since we are monitoring fluorescence changes of the sole YopH tryptophan located at the WPD loop, it is highly probable that the k_{open} and k_{close} values are close to the rates of loop opening and closing. This assumption will be verified in future UV−resonance Raman work.

From the thermodynamic parameters we conclude that, first, ligand binding stabilizes the closed form of the WPD loop; this stabilization is due to enthalpy. This is in contrast with the free enzyme where resonance Raman measurements show that the enzyme conformations associated "open" and "closed" forms have a similar stability (*11*). Second, the transition from open to closed forms of the WPD loop is not accompanied by any gain in entropy. This indicates that the open form of the WPD loop has not gained any additional degrees of freedom relative to the closed form. This is consistent with computational studies performed on YopHΔ162. These studies demonstrate that when the WPD loop is in the "open loop" conformation, it interacts with other segments of the protein that contribute to the stability of the open loop conformation (*59*). Third, the activation entropy is significant and negative. As the loop undergoes the open to close transition state, it passes through a highly ordered transition state. This may be because the transition state is more hydrated than the open and closed forms of the WPD loop (*60*).

Judging from our relaxation data, when YopHΔ162 is bound to ligand, the WPD loop opening/closing process occurs at a time scale of a few hundred microseconds. The T-jump relaxation profile that we obtain from the apoenzyme has a time constant of approximately 3 μs, as pointed out previously, this relaxation cannot be unambiguously assigned to loop motion of the enzyme. Juszczak et al. have suggested, on the basis of fluorescence anisotropy of the tryptophan of the WPD loop, that WPD loop closing and opening in the apoenzyme occurs at approximately 4 ns (*11*). On the basis of our T-jump data we believe this assignment to be unrealistic; time-resolved fluorescence anisotropy is difficult to interpret, and it is likely that the fast relaxation observed

by Juszczak et al. is a local relaxation of the indole ring rather than a collective motion of the ten amino acid residues forming the WPD loop. Future work will involve investigating the WPD loop motion in the apoenzyme with resonance Raman probed T-jump spectroscopy obtaining loop motion rates directly and unambiguously.

In summary we have characterized the mechanism in which small substrates bind to YopHΔ162. Small substrate binding is indeed well represented by the two step mechanism depicted in Scheme 1. The magnitudes of the different microscopic rate constants have been determined. We have directly demonstrated for the first time that all the substrate binding steps (including the WPD loop motion that brings the general acid Asp into the proximity of the substrate to initiate the first chemical step) can be considered to be "freely reversible" in solution. The enzyme demonstrates no sizable forward commitment for small substrates.

Finally, comparing the dynamic parameters the WPD loop motion of YopHΔ162 with those of the active site loop of triosephosphate isomerase (TIM) is informative (*33*). Both of these enzyme loops are located near the protein surface, and both have the same number of amino acids (~10). The dynamic rate constants for loop motion for both enzymes are within the same order of magnitude. The ratio between k_{close} and k_{open} at different temperatures varies between 10 and 20, and this ratio is rather insensitive to temperature. The energy difference between the closed and open states for both enzymes is less than 3RT, making both states thermodynamically accessible at room temperature. These values underline the fact that at room temperature enzymes (including the active site) are highly dynamic structures. Although certain enzymatic structures are imperative for catalysis, there is no "thermodynamic energy well" trapping the enzyme in a reactive conformation. Instead, the "catalytic structure" is only slightly favored thermodynamically, indicating that substrate binding is composed of a set of reversible equilibrium steps that lead to catalysis. TIM and YopHΔ162 however differ in one crucial aspect. Dynamic studies indicate that, for TIM, k_{cat} and k_{open} are very close to one another indicating that loop opening (i.e., substrate release) is the rate-limiting step of the catalytic cycle. In contrast, for the dephosphorylation of small tyrosine phosphates like PNPP by YopHΔ162, the dynamic processes occur much faster than the chemistry. This sluggish behavior of the chemical step may be due to the fact that PNPP is not the natural substrate of the enzyme. In fact, the catalysis rate of peptide tyrosine phosphates is faster than that of small unnatural substrates like PNPP. Future work will investigate the binding dynamics of peptide ligands to YopH and YopHΔ162.

REFERENCES

1. Neel, B. G., and Tonks, N. K. (1997) Protein tyrosine phosphatases in signal transduction, *Curr. Opin. Cell Biol. 9*, 193−204.
2. Zhang, Z. Y. (1998) Protein-tyrosine phosphatases: biological function, structural characteristics, and mechanism of catalysis, *Crit. Rev. Biochem. Mol. Biol. 33*, 1−52.
3. Kappert, K., Peters, K. G., Bohmer, F. D., and Ostman, A. (2005) Tyrosine phosphatases in vessel wall signaling, *Cardiovasc. Res. 65*, 587−98.
4. Jia, Z. (1997) Protein phosphatases: structures and implications, *Biochem. Cell Biol. 75*, 17−26.
5. Barford, D., Das, A. K., and Egloff, M. P. (1998) The structure and mechanism of protein phosphatases: insights into catalysis and regulation, *Annu. Rev. Biophys. Biomol. Struct. 27*, 133−64.
6. Stoker, A. W. (2005) Protein tyrosine phosphatases and signalling, *J. Endocrinol. 185*, 19−33.
7. Zhang, Z. Y. (2001) Protein tyrosine phosphatases: prospects for therapeutics, *Curr. Opin. Chem. Biol. 5*, 416−23.
8. van Huijsduijnen, R. H., Bombrun, A., and Swinnen, D. (2002) Selecting protein tyrosine phosphatases as drug targets, *Drug Discovery Today 7*, 1013−9.
9. Zhang, Z. Y. (2003) Chemical and mechanistic approaches to the study of protein tyrosine phosphatases, *Acc. Chem. Res. 36*, 385−92.
10. Yang, J., Niu, T., Zhang, A., Mishra, A. K., Zhao, Z. J., and Zhou, G. W. (2001) Relation between the flexibility of the WPD loop and the activity of the catalytic domain of protein tyrosine phosphatase SHP-1, *J. Cell. Biochem. 84*, 47−55.
11. Juszczak, L. J., Zhang, Z. Y., Wu, L., Gottfried, D. S., and Eads, D. D. (1997) Rapid loop dynamics of Yersinia protein tyrosine phosphatases, *Biochemistry 36*, 2227−36.
12. Zhang, Z. Y. (2002) Protein tyrosine phosphatases: structure and function, substrate specificity, and inhibitor development, *Annu. Rev. Pharmacol. Toxicol. 42*, 209−34.
13. Keng, Y. F., Wu, L., and Zhang, Z. Y. (1999) Probing the function of the conserved tryptophan in the flexible loop of the Yersinia protein-tyrosine phosphatase, *Eur. J. Biochem. 259*, 809−14.
14. Hoff, R. H., Hengge, A. C., Wu, L., Keng, Y. F., and Zhang, Z. Y. (2000) Effects on general acid catalysis from mutations of the invariant tryptophan and arginine residues in the protein tyrosine phosphatase from Yersinia, *Biochemistry 39*, 46−54.
15. Stuckey, J. A., Schubert, H. L., Fauman, E. B., Zhang, Z. Y., Dixon, J. E., and Saper, M. A. (1994) Crystal structure of Yersinia protein tyrosine phosphatase at 2.5 Å and the complex with tungstate, *Nature 370*, 571−5.
16. Sun, J. P., Wu, L., Fedorov, A. A., Almo, S. C., and Zhang, Z. Y. (2003) Crystal structure of the Yersinia protein-tyrosine phosphatase YopH complexed with a specific small molecule inhibitor, *J. Biol. Chem. 278*, 33392−9.
17. Hengge, A. C., Sowa, G. A., Wu, L., and Zhang, Z. Y. (1995) Nature of the transition state of the protein-tyrosine phosphatase-catalyzed reaction, *Biochemistry 34*, 13982−7.
18. Zhang, Z. Y., Palfey, B. A., Wu, L., and Zhao, Y. (1995) Catalytic function of the conserved hydroxyl group in the protein tyrosine phosphatase signature motif, *Biochemistry 34*, 16389−96.
19. Zhang, Z. Y. (1995) Kinetic and mechanistic characterization of a mammalian protein-tyrosine phosphatase, PTP1, *J. Biol. Chem. 270*, 11199−204.
20. Zhang, Z. Y., Clemens, J. C., Schubert, H. L., Stuckey, J. A., Fischer, M. W., Hume, D. M., Saper, M. A., and Dixon, J. E. (1992) Expression, purification, and physicochemical characterization of a recombinant Yersinia protein tyrosine phosphatase, *J. Biol. Chem. 267*, 23759−66.
21. Hengge, A. C., Zhao, Y., Wu, L., and Zhang, Z. Y. (1997) Examination of the transition state of the low-molecular mass small tyrosine phosphatase 1. Comparisons with other protein phosphatases, *Biochemistry 36*, 7928−36.
22. Khandelwal, P., Keliikuli, K., Smith, C. L., Saper, M. A., and Zuiderweg, E. R. (2002) Solution structure and phosphopeptide binding to the N-terminal domain of Yersinia YopH: comparison with a crystal structure, *Biochemistry 41*, 11425−37.
23. Evdokimov, A. G., Tropea, J. E., Routzahn, K. M., Copeland, T. D., and Waugh, D. S. (2001) Structure of the N-terminal domain of Yersinia pestis YopH at 2.0 Å resolution, *Acta Crystallogr., Sect. D: Biol. Crystallogr. 57*, 793−9.
24. Gandour, R. D., and Schowen, R. L. (1987) *Transition States of Biochemical Processes*, Plenum Press, New York.
25. Fersht, A. (1985) *Enzyme Structure and Mechanism*, Freeman & Co., New York.
26. Falzone, C. J., Wright, P. E., and Benkovic, S. J. (1994) Dynamics of a flexible loop in dihydrofolate reductase from Escherichia coli and its implication for catalysis, *Biochemistry 33*, 439−42.
27. Wang, G. P., Cahill, S. M., Liu, X., Girvin, M. E., and Grubmeyer, C. (1999) Motional dynamics of the catalytic loop in OMP synthase, *Biochemistry 38*, 284−95.
28. Waldman, A. D., Hart, K. W., Clarke, A. R., Wigley, D. B., Barstow, D. A., Atkinson, T., Chia, W. N., and Holbrook, J. J. (1988) The use of genetically engineered tryptophan to identify the movement of a domain of B. stearothermophilus lactate dehydrogenase with the process which limits the steady-state turnover of the enzyme, *Biochem. Biophys. Res. Commun. 150*, 752−9.

29. Ito, Y., Yamasaki, K., Iwahara, J., Terada, T., Kamiya, A., Shirouzu, M., Muto, Y., Kawai, G., Yokoyama, S., Laue, E. D., Walchli, M., Shibata, T., Nishimura, S., and Miyazawa, T. (1997) Regional polysterism in the GTP-bound form of the human c-Ha-Ras protein, *Biochemistry 36*, 9109−19.
30. Rozovsky, S., Jogl, G., Tong, L., and McDermott, A. E. (2001) Solution-state NMR investigations of triosephosphate isomerase active site loop motion: ligand release in relation to active site loop dynamics, *J. Mol. Biol. 310*, 271−80.
31. Rozovsky, S., Kaizuka, Y., and Groves, J. T. (2005) Formation and spatio-temporal evolution of periodic structures in lipid bilayers, *J. Am. Chem. Soc. 127*, 36−7.
32. Rozovsky, S., and McDermott, A. E. (2001) The time scale of the catalytic loop motion in triosephosphate isomerase, *J. Mol. Biol. 310*, 259−70.
33. Desamero, R., Rozovsky, S., Zhadin, N., McDermott, A., and Callender, R. (2003) Active site loop motion in triosephosphate isomerase: T-jump relaxation spectroscopy of thermal activation, *Biochemistry 42*, 2941−51.
34. Callender, R., and Dyer, R. B. (2002) Probing protein dynamics using temperature jump relaxation spectroscopy, *Curr. Opin. Struct. Biol. 12*, 628−33.
35. McClendon, S., Zhadin, N., and Callender, R. (2005) The approach to the Michaelis complex in lactate dehydrogenase: the substrate binding pathway, *Biophys. J. 89*, 2024−32.
36. McClendon, S., Vu, D. M., Clinch, K., Callender, R., and Dyer, R. B. (2005) Structural transformations in the dynamics of Michaelis complex formation in lactate dehydrogenase, *Biophys. J. 89*, L07−9.
37. Gulotta, M., Deng, H., Dyer, R. B., and Callender, R. H. (2002) Toward an understanding of the role of dynamics on enzymatic catalysis in lactate dehydrogenase, *Biochemistry 41*, 3353−63.
38. Deng, H., Zhadin, N., and Callender, R. (2001) Dynamics of protein ligand binding on multiple time scales: NADH binding to lactate dehydrogenase, *Biochemistry 40*, 3767−73.
39. Schubert, H. L., Fauman, E. B., Stuckey, J. A., Dixon, J. E., and Saper, M. A. (1995) A ligand-induced conformational change in the Yersinia protein tyrosine phosphatase, *Protein Sci. 4*, 1904−13.
40. Eigen, M. (1968) New looks and outlooks on physical enzymology, *Q. Rev. Biophys. 1*, 3−33.
41. Yapel, A. F., Jr. (1971) A practical guide to the temperature-jump method for measuring the rate of fast reactions, *Methods Biochem. Anal. 20*, 169−350.
42. Eigen, M., and Hammes, G. G. (1963) Elementary Steps in Enzyme Reactions (as Studied by Relaxation Spectrometry), *Adv. Enzymol. Relat. Areas Mol. Biol. 25*, 1−38.
43. Eigen, M., and De Maeyer, L. D. (1963) Relaxation Methods, in *Techniques of Organic Chemistry* (Friess, S. L., Lewis, E. S., and Weissberger, A., Eds.) pp 895−1054, Interscience, New York.
44. Hammes, G. G. (1968) Relaxation spectrometry of biological systems, *Adv. Protein Chem. 23*, 1−57.
45. Fasella, P., and Hammes, G. G. (1967) A. temperature jump study of aspartate aminotransferase. A reinvestigation, *Biochemistry 6*, 1798−804.
46. Malcolm, A. D. (1972) Temperature-jump studies on glutamate dehydrogenase, *Biochem. J. 128*, 98P.
47. Wilson, M. T., Greenwood, C., Brunori, M., and Antonini, E. (1975) Electron transfer between azurin and cytochrone c-551 from Pseudomonas aeruginosa, *Biochem. J. 145*, 449−57.
48. Baldo, J. H., Halford, S. E., Patt, S. L., and Sykes, B. D. (1975) The stepwise binding of small molecules to proteins. Nuclear magnetic resonance and temperature jump studies of the binding of 4-(N-acetylaminoglucosyl)-N-acetylglucosamine to lysozyme, *Biochemistry 14*, 1893−9.
49. Koren, R., and Hammes, G. G. (1976) A kinetic study of protein-protein interactions, *Biochemistry 15*, 1165−71.
50. Rosenberry, T. L., and Neumann, E. (1977) Interaction of ligands with acetylcholinesterase. Use of temperature-jump relaxation kinetics in the binding of specific fluorescent ligands, *Biochemistry 16*, 3870−8.
51. Vandenbunder, B., Dreyfus, M., and Buc, H. (1978) Conformational changes and local events at the AMP site of glycogen phosphorylase b: a fluorescence temperature-jump relaxation study, *Biochemistry 17*, 4153−60.
52. Williams, S., Causgrove, T. P., Gilmanshin, R., Fang, K. S., Callender, R. H., Woodruff, W. H., and Dyer, R. B. (1996) Fast events in protein folding: helix melting and formation in a small peptide, *Biochemistry 35*, 691−7.
53. Gulotta, M., Gilmanshin, R., Buscher, T. C., Callender, R. H., and Dyer, R. B. (2001) Core formation in apomyoglobin: probing the upper reaches of the folding energy landscape, *Biochemistry 40*, 5137−43.
54. van Holde, K. E., Johnson, W. C., and Ho, S. H. (1998) *Principles of Physical Biochemistry*, Prentice Hall, Upper Saddle River, NJ.
55. Lakowicz, J. R. (1999) *Principles of Fluorescence Spectroscopy*, Kluwer Academic/Plenum Publishers, New York.
56. Halford, S. E. (1972) Escherichia coli alkaline phosphatase. Relaxation spectra of ligand binding, *Biochem. J. 126*, 727−38.
57. Zhang, Z. Y., Malachowski, W. P., Van Etten, R. L., and Dixon, J. E. (1994) Nature of the rate-determining steps of the reaction catalyzed by the Yersinia protein-tyrosine phosphatase, *J. Biol. Chem. 269*, 8140−5.
58. Hengge, A. C., Denu, J. M., and Dixon, J. E. (1996) Transition-state structures for the native dual-specific phosphatase VHR and D92N and S131A mutants. Contributions to the driving force for catalysis, *Biochemistry 35*, 7084−92.
59. Hu, X., and Stebbins, C. E. (2006) Dynamics of the WPD loop of the Yersinia protein tyrosine phosphatase, *Biophys. J. 91*, 948−56.
60. Privalov, P. L., and Makhatadze, G. I. (1993) Contribution of hydration to protein folding thermodynamics. II. The entropy and Gibbs energy of hydration, *J. Mol. Biol. 232*, 660−79.
61. Robinson, D., Smith, J. N., Spencer, B., and Williams, R. T. (1952) Studies in detoxication. XXXXIII. A study of the arylsulphatase activity of takadiastase towards some phenolic ethereal sulphates, *Biochem. J. 51*, 202−8.

BI602335X